Nanostructured Semiconductor Films for Photocatalysis. Photoelectrochemical Behavior of SnO_2/TiO_2 Composite Systems and Its Role in Photocatalytic Degradation of a Textile Azo Dye

K. Vinodgopal,*,† Idriss Bedja,‡,§ and Prashant V. Kamat*,‡

Department of Chemistry, Indiana University Northwest, Gary, Indiana 46408, and Radiation Laboratory, University of Notre Dame, Notre Dame, Indiana 46556

Received September 12, 1995. Revised Manuscript Received April 8, 1996⊗

Nanostructured semiconductor films of SnO_2, TiO_2 and SnO_2/TiO_2 have been employed for *electrochemically assisted* photocatalytic degradation of a textile azo dye naphthol blue black (NBB). The degradation rate is significantly higher for SnO_2/TiO_2 composite films than SnO_2 and TiO_2 films alone. An effort has been made to correlate the photoelectrochemical behavior of these films to the rate of photocatalytic degradation of NBB. The enhanced degradation rate of NBB using composite semiconductor films is attributed to increased charge separation in these systems. Photoelectrochemical and photocatalytic degradation experiments carried out in both nitrogen- and oxygen-saturated solutions with an externally applied electrochemical bias provide useful information in optimizing semiconductor concentrations in a composite film.

Introduction

Photocatalytic degradation of several organic contaminants using large-bandgap semiconductor particles suspended in aqueous solutions as well as immobilized semiconductor films has been studied extensively.[1−19] Hydroxyl radicals generated following the oxidation of hydroxide ions by photogenerated holes are the major oxidizing species in photocatalysis.[8,20−25] In slurry-based photocatalytic reactor systems, the rate-determining step in the degradation process is considered to be the reduction of oxygen by the trapped electrons on the semiconductor surface to produce reduced oxygen species such as the superoxide radical ion O_2^- or H_2O_2.[25−32] Failure to scavenge electrons with a sacrificial electron-acceptor results in the promotion of charge recombination. Alternative methods have also been suggested to promote charge separation by applying an electrochemical bias to a TiO_2 particulate film electrode.[13,24,30,33,34]

† Indiana University Northwest (e-mail: KVinod@iunhaw1.iun.indiana.edu).

‡ University of Notre Dame (e-mail: Kamat.1@nd.edu).

§ Permanent address: Centre de Recherche en Photobiophysique, Université du Québec à Trois Rivières, Trois Rivières, Québec, G9A 5H7, Canada.

⊗ Abstract published in *Advance ACS Abstracts,* July 15, 1996.

(1) Bard, A. J. *J. Photochem.* **1979**, *10*, 59.
(2) Kalyanasundaram, K.; Grätzel, M. *Springer Ser. Chem. Phys.* **1984**, *39*.
(3) Fox, M. A. *Chemtech* **1992**, *22*, 680.
(4) Ollis, D. F. *Environ. Sci. Technol.* **1985**, *19*, 480.
(5) Ollis, D. F.; Pelizzetti, E.; Serpone, N. In *Photocatalysis. Fundamentals and Applications*; Serpone, N., Pelizzetti, E., Eds.; Wiley: New York, 1989; p 603.
(6) *Photocatalysis. Fundamentals and Applications*; Serpone, N., Pelizzetti, E., Eds.; John Wiley and Sons: New York, 1989; p 650.
(7) Kamat, P. V. In *Kinetics and Catalysis in Microheterogeneous Systems*; Grätzel, M., Kalyanasundaram, K., Eds.; Marcel Dekker, Inc.: New York, 1991; p 375.
(8) Ollis, D. F.; Pelizzetti, E.; Serpone, N. *Environ. Sci. Technol.* **1991**, *25*, 1523.
(9) Herrmann, J. M.; Guillard, C.; Pichat, P. *Catal. Today* **1993**, *17*, 7.
(10) Vinodgopal, K.; Kamat, P. V. In *Aquatic and Surface Photochemistry*; Helz, G. R., Zepp, R. G., Crosby, D. G., Eds.; CRC Press, Inc.: Boca Raton, FL, 1994; p 437.
(11) Kamat, P. V.; Vinodgopal, K. In *Photocatalytic Purification and Treatment of Water and Air*; Ollis, D. F., Al-Ekabi, H., Eds.; Elsevier Science Publishers B.V.: Amsterdam, The Netherlands, 1993; p 8.
(12) Kamat, P. V. *Chem. Rev.* **1993**, *93*, 267.
(13) Zeltner, W. A.; Hill, C. G., Jr.; Anderson, M. A. *Chem. Technol.* **1994**, 21.
(14) Bahnemann, D.; Cunningham, J.; Fox, M. A.; Pelizzetti, E.; Pichat, P.; Serpone, N. In *Aquatic and Surface Chemistry*; Helz, G. R., Zepp, R. G., Crosby, D. G., Eds.; Lewis Publishers: Boca Raton, FL, 1994; p 261.
(15) Rajeshwar, K. *J. Appl. Electrochem.* **1995**, *25*, 1067.
(16) Stafford, U.; Gray, K. A.; Kamat, P. V. *Heterogeneous Chem. Rev.*, in press.
(17) Hoffmann, M. R.; Martin, S. T.; Choi, W.; Bahnemann, D. W. *Chem. Rev.* **1995**, *95*, 69.
(18) Kamat, P. V. In *Molecular level artificial photosynthetic materials. Progress in Inorganic Chemistry Series*; Meyer, J., Ed.; John Wiley & Sons, Inc.: New York, 1996; Vol. 44, in press.
(19) Linsebigler, A. L.; Lu, G.; Yates, J. J. T. *Chem. Rev.* **1995**, *95*, 735.
(20) Jaeger, C. D.; Bard, A. J. *J. Phys. Chem.* **1979**, *83*, 3146.
(21) Anpo, M.; Shima, T.; Kubokawa, Y. *Chem. Lett.* **1985**, 1799.
(22) Matthews, R. W. *J. Phys. Chem.* **1987**, *91*, 3328.
(23) Fox, M. A. In *Photocatalytic Purification and Treatment of Water and Air*; Ollis, D. F., Al-Ekabi, H., Eds.; Elsevier Science Publishers B.V.: Amsterdam, Netherlands, 1993; p 8.
(24) Vinodgopal, K.; Stafford, U.; Gray, K. A.; Kamat, P. V. *J. Phys. Chem.* **1994**, *98*, 6797.
(25) Stafford, U.; Gray, K. A.; Kamat, P. V. In *Chemical Oxidation: Technology for the 90*'s; Roth, J., Bowers, A., Eds.; Technomics: Lancaster, PA, 1995; Vol. 4, in press.
(26) Gerischer, H.; Heller, A. *J. Phys. Chem.* **1991**, *95*, 5261.
(27) Wang, C. M.; Heller, A.; Gerischer, H. *J. Am. Chem. Soc.* **1992**, *114*, 5230.
(28) Gerischer, H.; Heller, A. *J. Electrochem. Soc.* **1992**, *139*, 113.
(29) Peterson, M. W.; Turner, J. A.; Nozik, A. J. *J. Phys. Chem.* **1991**, *95*, 221.
(30) Vinodgopal, K.; Hotchandani, S.; Kamat, P. V. *J. Phys. Chem.* **1993**, *97*, 9040.
(31) Kesselman, J. M.; Kumar, A.; Lewis, N. S. In *Photocatalytic Purification and Treatment of Water and Air*; Ollis, D. F., Al-Ekabi, H., Eds.; Elsevier Science Publishers B.V.: Amsterdam, 1993; p 19.
(32) Kesselman, J. M.; Shreve, G. A.; Hoffmann, M. R.; Lewis, N. S. *J. Phys. Chem.* **1994**, *98*, 13385.
(33) Kim, D. H.; Anderson, M. A. *Environ. Sci. Technol.* **1994**, *28*, 479.
(34) Hidaka, H.; Asai, Y.; Zhao, J.; Nohara, K.; Pelizzetti, E.; Serpone, N. *J. Phys. Chem.* **1995**, *99*, 8244.

S0897-4756(95)00425-X CCC: $12.00

Suppression of the recombination of photogenerated charge carriers in a semiconductor particulate system is essential for improving the efficiency of net charge transfer at the semiconductor/electrolyte interface (see for example refs 12 and 35−38). Simultaneous scavenging of holes and electrons by surface-adsorbed redox species have been shown to improve the efficiency of interfacial charge transfer.[39,40] Another interesting approach involves coupling of two semiconductor particles with different energy levels. A variety of semiconductor heterojunctions has been investigated in colloidal suspensions following the concept of a photochemical diode put forth by Nozik and co-workers.[41] These include CdS/TiO_2,[42−44] CdS/PbS,[45] CdS/ZnO,[43,46] CdS/AgI,[44] Cd_3P_2/TiO_2 and Cd_3P_2/ZnO,[47] and AgI/Ag_2S.[48] Recently, efforts are also being made to develop capped semiconductor systems with a core-shell geometry (e.g., ZnO/ZnS,[49] ZnO/TiO_2,[50] ZnO/ZnSe,[51] CdS/HgS,[52] and SnO_2/TiO_2[53]).

In our earlier studies we have shown that excitation of CdS colloids coupled with a metal oxide colloid such as TiO_2[44] or ZnO[46] results in the injection of electrons into the lower lying conduction band of the metal oxide. The charge injection process in these systems was shown to occur within the pulse duration of 20 ps. Recent studies have indicated that such an interparticle electron transfer occurs within 0.5−2 ps.[54,55] Use of coupled semiconductor particles in improving the photocurrent generation in a thin TiO_2/CdS,[56−59] ZnO/CdS,[46] and TiO_2/CdSe[60,61] nanocrystalline film has also been demonstrated. These composite semiconductor thin films not only extend the photoresponse of large-bandgap semiconductors but also rectify the flow of photogenerated charge carriers[60] and improve the efficiency of dye sensitization.[62]

Scheme 1. Idealized Illustration of Photoinduced Charge Separation in a Composite Semiconductor Film

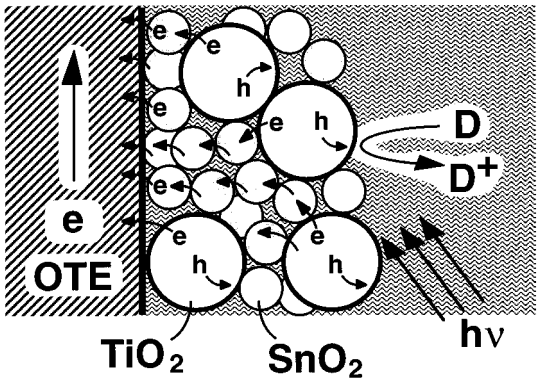

Efforts have been made to employ mixed semiconductor slurries for photocatalytic degradation of organic compounds.[42,63] Recently, we have demonstrated that a significant enhancement in the photocatalytic degradation rate of acid orange 7 can be achieved by employing SnO_2 and TiO_2 nanoclusters in the composite film.[64] Since the conduction band (CB) of SnO_2 (E_{CB} for SnO_2 = 0 V vs NHE at pH 7) is lower than that of the TiO_2 (E_{CB} = −0.5V vs NHE at pH 7) the former acts as a sink for the photogenerated electrons. The holes move in the opposite direction from the electrons and accumulate on the TiO_2 particle, thereby making charge separation more efficient. Our particular success in improving the efficiency of photocatalytic degradation can be attributed to the fact that we deposit these nanostructured films on an optically transparent electrode (OTE) and transport the electrons efficiently to the external circuit with an externally applied electrochemical bias.[24,30] The principle of charge separation in such a composite semiconductor system deposited on an OTE is shown in Scheme 1. Unlike in slurry systems, the photocatalytic degradation experiments can be carried out in the absence of electron scavengers such as O_2. By employing a two-compartment electrochemical cell, we have now investigated the photocatalytic degradation of a textile azo dye, naphthol blue black (NBB).

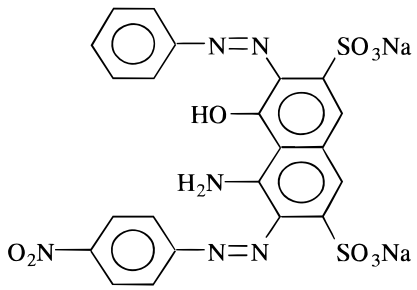

Azo dyes are ubiquitous commercial chemicals that present unique environmental problems.[65−68] More

(35) Kalyanasundaram, K.; Grätzel, M.; Pelizzetti, E. *Coord. Chem. Rev.* **1986**, *69*, 57.
(36) Henglein, A. *Chem. Rev.* **1989**, *89*, 1861.
(37) Weller, H. *Angew. Chem., Int. Ed. Engl.* **1993**, *32*, 41.
(38) Kamat, P. V. *Prog. React. Kinet.* **1994**, *19*, 277.
(39) Bahnemann, D.; Henglein, A.; Spanhel, L. *Faraday Discuss. Chem. Soc* **1984**, *78*, 151.
(40) Kamat, P. V. *Langmuir* **1985**, *1*, 608.
(41) Nozik, A. J. *Appl. Phys. Lett.* **1977**, *30*, 567.
(42) Serpone, N.; Borgarello, E.; Grätzel, M. *J. Chem. Soc., Chem. Commun.* **1984**, 342.
(43) Spanhel, L.; Weller, H.; Henglein, A. *J. Am. Chem. Soc.* **1987**, *109*, 6632.
(44) Gopidas, K. R.; Bohorquez, M.; Kamat, P. V. *J. Phys. Chem.* **1990**, *94*, 6435.
(45) Zhou, H. S.; Honma, I.; Komiyama, H. *J. Phys. Chem.* **1993**, *97*, 895.
(46) Hotchandani, S.; Kamat, P. V. *J. Phys. Chem.* **1992**, *96*, 6834.
(47) Spanhel, L.; Henglein, A.; Weller, H. *Ber. Bunsen-Ges. Phys. Chem.* **1987**, *91*, 1359.
(48) Henglein, A.; Gutierrez, M.; Weller, H.; Fojtik, A.; Jirkovsky, J. *Ber. Bunsen-Ges. Phys. Chem.* **1989**, *93*, 593.
(49) Rabani, J. *J. Phys. Chem.* **1989**, *93*, 7707.
(50) Ocana, M.; Hsu, W. P.; Matijevic, E. *Langmuir* **1991**, *7*, 2911.
(51) Kamat, P. V.; Patrick, B. *J. Phys. Chem.* **1992**, *96*, 6829.
(52) Haesselbarth, A.; Eychmueller, A.; Eichberger, R.; Giersig, M.; Mews, A.; Weller, H. *J. Phys. Chem.* **1993**, *97*, 5333.
(53) Bedja, I.; Kamat, P. V. *J. Phys. Chem.* **1995**, *99*, 9182.
(54) Kietzmann, R.; Willig, F.; Weller, H.; Vogel, R.; Nath, D. N.; Eichberger, R.; Liska, P.; Lehnert, J. *Mol. Cryst. Liq. Cryst.* **1991**, *194*, 169.
(55) Evans, J. E.; Springer, K. W.; Zhang, J. Z. *J. Chem. Phys.* **1994**, *101*, 6222.
(56) Gerischer, H.; Luebke, M. *J. Electroanal. Chem. Interfacial Electrochem.* **1986**, *204*, 225.
(57) Vogel, R.; Pohl, K.; Weller, H. *Chem. Phys. Lett.* **1990**, *174*, 241.
(58) Kohtani, S.; Kudo, A.; Sakata, T. *Chem. Phys. Lett.* **1993**, *206*, 166.
(59) Vogel, R.; Hoyer, P.; Weller, H. *J. Phys. Chem.* **1994**, *98*, 3183.
(60) Liu, D.; Kamat, P. V. *J. Phys. Chem.* **1993**, *97*, 10769.
(61) Liu, D.; Kamat, P. V. *J. Electroanal. Chem. Interfacial Electrochem.* **1993**, *347*, 451.
(62) Hotchandani, S.; Kamat, P. V. *Chem. Phys. Lett.* **1992**, *191*, 320.
(63) Serpone, N.; Maruthamuthu, P.; Pichat, P.; Pelizzetti, E.; Hidaka, H. *J. Photochem. Photobiol., A: Chem.* **1995**, *85*, 247.
(64) Vinodgopal, K.; Kamat, P. V. *Environ. Sci. Technol.* **1995**, *29*, 841.
(65) Vaidya, A. A.; Datye, K. V. *Colourage* **1982**, *14*, 3.
(66) Zollinger, H. *Color Chemistry: Synthesis, Properties and Applications of Organic Dyes and Pigments*; VCH Publishers: New York, 1987.

than 300 million pounds of dyes are produced annually in the U.S.A. Colored dye effluents pose a major problem for the manufacturing plant as well as water-treatment plants downstream.[69] Quite apart from the aesthetic desirability of colored streams resulting from dye waste, the azo dyes in particular can undergo natural anaerobic degradation to potentially carcinogenic amines.[68]

In the present study we have measured photoelectrochemical properties of the composite SnO_2/TiO_2 films under both nitrogen- and oxygen-saturated conditions and as a function of varying composition. These properties are useful for understanding enhanced photocatalytic activity of these composite systems vis-à-vis the degradation of a common commercial azo dye such as NBB.

Experimental Section

Materials and Electrode Preparation. Naphthol blue black (NBB) was obtained from Aldrich and purified with column chromatography using a neutral alumina column and ethyl acetate, ethanol, and water as eluents. Optically transparent electrodes (OTE) were cut from a conducting glass plate obtained from Donelley Corporation, Holland, MI. TiO_2 powder (product name P-25, particle diameter 30 nm, surface area 50 m^2/g) was a gift sample from Degussa Corp. SnO_2 colloidal suspension (18%) was obtained from Alfa Chemicals. The diameter of the SnO_2 colloidal particle is 3−5 nm. The TiO_2 particulate film was prepared by applying 0.25 mL of TiO_2 slurry (1.64 g TiO_2/L water) to half the area of OTE plate (5 cm × 0.9 cm). The TiO_2 loading corresponds to 6.6 mg of TiO_2 spread on an area of approximately 2.2 cm^2 of the OTE plate. In a similar way diluted suspension (2%) of SnO_2 colloids was applied to OTE plate. Composite films of SnO_2/TiO_2 were prepared by mixing the two colloid suspensions at the desired ratio with sonication and applying it to the conducting surface of OTE. After air drying on a warm plate all these films were annealed at 673 K. The uncovered area of the OTE plate was used to make the electrical contact. These electrodes with immobilized TiO_2 (referred to as OTE/TiO_2), SnO_2 (OTE/SnO_2), and composite semiconductor (OTE/SnO_2/TiO_2) films were directly employed as a working electrode in the electrochemical cell.

A Hitachi S-4500 scanning electron microscope (SEM) was employed to record the images of the nanostructured semiconductor films with either 150 or 200 K magnifications. The films were cast on conducting glass substrates (1 cm^2) using the procedure described above.

Photoelectrochemical and Photocatalytic Experiments. Unless otherwise specified, all the electrochemical and photoelectrochemical measurements were carried out in a standard two-compartment cell in which working and counter electrodes were separated by a fine glass frit. The electrode assembly consisted of a semiconductor film coated OTE working electrode, a platinum wire gauze counter electrode and a saturated calomel reference electrode (SCE). The evaluation of the nanostructured film was performed in an alkaline medium (0.02 M NaOH), while all the photocatalytic experiments were performed in an unbuffered aqueous medium.

The initial pH of a 1 mM NBB solution employed in the photocatalysis experiment was between 4 and 5. After the photocatalytic degradation of the dye the pH of the solution dropped to 2.5. (Please note that the solution pH (2−6) has no effect on the absorption spectrum of NBB.) The N_2 and O_2 atmospheres in individual compartments were maintained by purging individual gases with a slow stream separately in the two compartments during the operation of the cell. The total volume of the dye solution in the working electrode compartment was 7 mL. The dye degradation was monitored from the disappearance of the visible absorption band.

A Princeton Applied Research (PAR) Model 173 potentiostat and Model 175 universal programmer and Bioanalytical Systems (BAS) 100 Electrochemical Analyzer was used in all the electrochemical measurements. Photocurrent measurements were carried out with a Keithley Model 617 programmable electrometer. All measurements were carried out at room temperature (∼296 K). A collimated light beam from a 250 W xenon lamp was used for excitation of the electrode in the front face (electrolyte side) configuration. To ensure selective excitation of the semiconductor film (λ > 300 nm), a 10-cm long $CuSO_4$ solution filter was placed in the optical path. A Bausch and Lomb monochromator (slit width ∼4 mm) was introduced in the optical path for obtaining monochromatic light during wavelength-dependent photocurrent measurements. (A band spread of ±5 nm can be expected at these settings.) The incident intensity at the cell position was separately measured with a pyroelectric sensor (laser Precision Corp. RJP-735).

Results and Discussion

SEM Characterization. The scanning electron micrographs of TiO_2, SnO_2, and SnO_2/TiO_2 particulate films are shown in Figure 1. The particle diameter of TiO_2 and SnO_2 colloids employed for casting these films were ∼30 and ∼5 nm, respectively. The pictures in Figure 1a,b show no significant change in particle size in annealed films except for clustering in a random fashion. The *grape bunch*-type clusters create nanostructured pores of various dimensions within the film. It is interesting to note that the individual spherical particles of TiO_2 (∼30 nm diameter in Figure 1a) and SnO_2 (∼5 nm diameter in Figure 1b) could still be visualized from these SEM pictures. Although there is no definite ordering of these aggregates in these films the three dimensional network of semiconductor nanoclusters provides a highly porous morphology. Thus a large surface area becomes available for initiating photocatalytic redox processes in these semiconductor thin films. In the case of SnO_2/TiO_2 composite films (Figure 1c), a distribution of smaller size SnO_2 particles on the TiO_2 particles could be seen. Because of the difference in size, several SnO_2 particles are capable of interacting with a single TiO_2 particle. Such a direct contact between the two particles has been found to be crucial for improving the photocatalytic activity of the composite semiconductor films.

Photoelectrochemical Properties of OTE/TiO_2 OTE/SnO_2 and OTE/SnO_2/TiO_2 Electrodes. The immobilized particles on the OTE surface are photoactive and collectively yield anodic photocurrent similar to that of an n-type semiconductor material.[30,60,70−73] The charge separation in these immobilized particles is controlled by the differing rates of electron and hole injection into the electrolyte and can be directly controlled with the application of an anodic bias.

The photoelectrochemical response and absorption spectra of the SnO_2, TiO_2, and SnO_2/TiO_2 nanoclusters immobilized on a conducting glass surface are shown in Figure 2. The incident photon-to-photocurrent ef-

(67) McCann, J.; Ames, B. N. *Proc. Natl. Acad. Sci. U.S.A.* **1975**, *73*, 950.
(68) Tincher, W. C. *Textile Chem. Colorist* **1989**, *21*, 33.
(69) Boeninger, M. *DHHS (NIOSH)* **1990**, *Publication No 80*, 119.
(70) Hodes, G.; Howell, I. D. J.; Peter, L. M. *J. Electrochem. Soc.* **1992**, *139*, 3136.
(71) Bedja, I.; Hotchandani, S.; Kamat, P. V. *J. Phys. Chem.* **1994**, *98*, 4133.
(72) Hagfeldt, A.; Lindquist, S. E.; Grätzel, M. *Sol. Energy Mater. Sol. Cells* **1994**, *32*, 245.
(73) Sodergren, S.; Hagfeldt, A.; Olsson, J.; Lindquist, S.-E. *J. Phys. Chem.* **1994**, *98*, 5552.

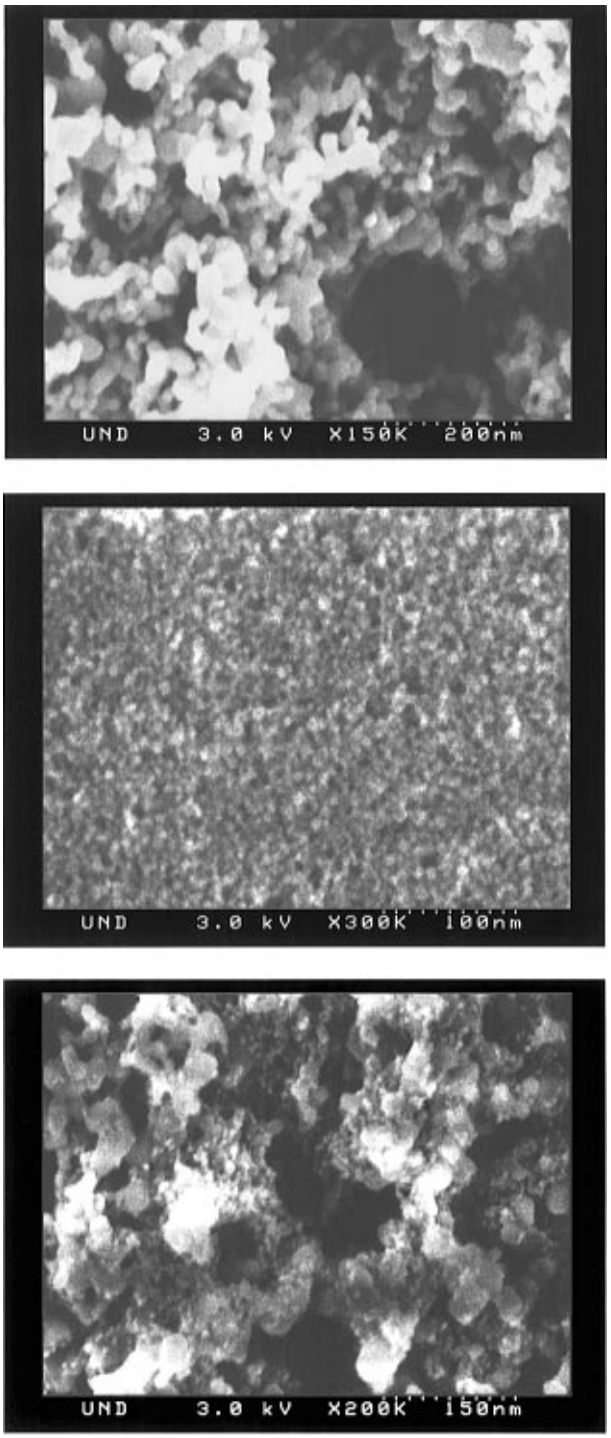

Figure 1. Scanning electron micrographs of semiconductor particulate films of (a, top), TiO_2, (b, middle), SnO_2, and (c, bottom) SnO_2/TiO_2 cast on a conducting glass substrate. These pictures were recorded with magnifications of (a) 150, (b) 300, and (c) 200 K, respectively. (The ratio of SnO_2 and TiO_2 in the composite film was 1:1.)

ficiency (IPCE) was determined by measuring the photocurrent of OTE/TiO_2 electrode at various excitation wavelengths and using the expression

$$\text{IPCE (\%)} = 100 \times (1240 \times i_{sc})/(\lambda \times I_{inc}) \qquad (1)$$

where i_{sc} is the short-circuit current photocurrent (A/cm^2), I_{inc} is the incident light intensity (W/cm^2), and λ is the excitation wavelength (nm). The onset of photocurrent is seen at the wavelengths ~360 and ~400 nm for SnO_2 and TiO_2 films, respectively. The increase in the photocurrent at excitation wavelengths below this

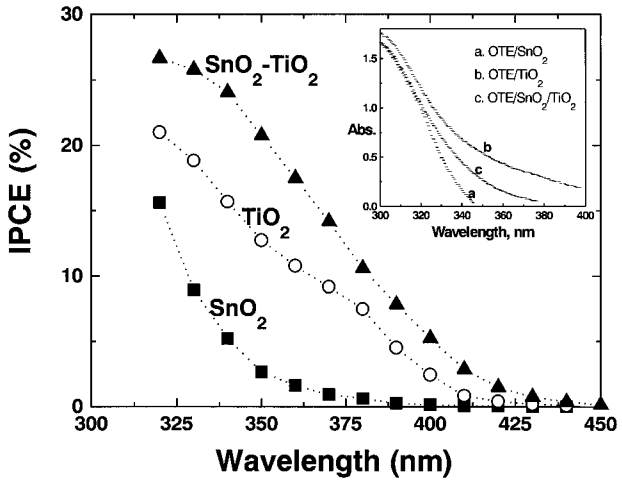

Figure 2. Photocurrent action spectrum of (a) OTE/SnO_2, (■), (b) OTE/TiO_2 (○); and (c) OTE/SnO_2/TiO_2 (▲) electrode in deaerated 0.02 M NaOH. (Excitation source: monochromatic light from the xenon lamp. The electrodes were maintained at a bias potential of 0.8 V. The composition of composite semiconductor film was 0.18 mg/cm^2 of SnO_2 and 0.18 mg/cm^2 of TiO_2.) See eq 1 for the analysis of IPCE. The absorption spectra of the corresponding electrodes are shown in the inset.

onset wavelength closely matches the absorption characteristics of SnO_2 (E_g = 3.5 eV) and anatase TiO_2 (E_g = 3.2 eV). This indicates that the observed photocurrent is initiated by the excitation of semiconductor nanoclusters in the thin film. The composite film, OTE/SnO_2/TiO_2, exhibited higher IPCE than OTE/SnO_2 or OTE/TiO_2. A maximum IPCE of ~25% was obtained at 325 nm. Since the absorption of the SnO_2/TiO_2 composite film in the 300−400 nm region was lower than that of the TiO_2 film, the increased IPCE cannot be attributed to the increase in light absorption. The higher IPCE of the OTE/SnO_2/TiO_2 electrode is therefore suggestive of increased charge separation in the composite film. The generation of anodic current is also indicative of the fact that the direction of flow of electrons is towards the OTE surface.

Photovoltage−Time Response. The photoresponse of OTE/SnO_2/TiO_2 is compared with the OTE/SnO_2 and OTE/TiO_2 electrodes in Figure 3. The photovoltage−time responses were recorded in both N_2- and O_2-saturated solutions. Upon illumination of these electrodes with bandgap excitation, the photogenerated electrons are trapped within the semiconductor nanoclusters, thereby shifting the pseudo-Fermi level (E_f') of the semiconductor film. The difference in energy between E_f' and the oxidation potential of the redox couple corresponds to the maximum voltage that one can expect in such nanostructured films. In the present study the maximum photovoltage observed for OTE/TiO_2 is ~800 mV, while that for OTE/SnO_2 is ~500 mV in N_2-saturated solutions.

However, in O_2-saturated solutions, the electron accumulation is less efficient as surface-adsorbed oxygen scavenges the photogenerated electrons. This effect is readily seen in the case of TiO_2 films as the photovoltage decays more rapidly in O_2-saturated solutions. However, adsorbed O_2 had a relatively small effect on the photovoltages generated at SnO_2 and SnO_2/TiO_2 composite films. This suggests that electrons accumulated within SnO_2 particles are not likely to be reduced by O_2 because of the unfavorable energetics. The conduction band electrons in SnO_2 (E_{CB} = 0.0 V vs NHE), being

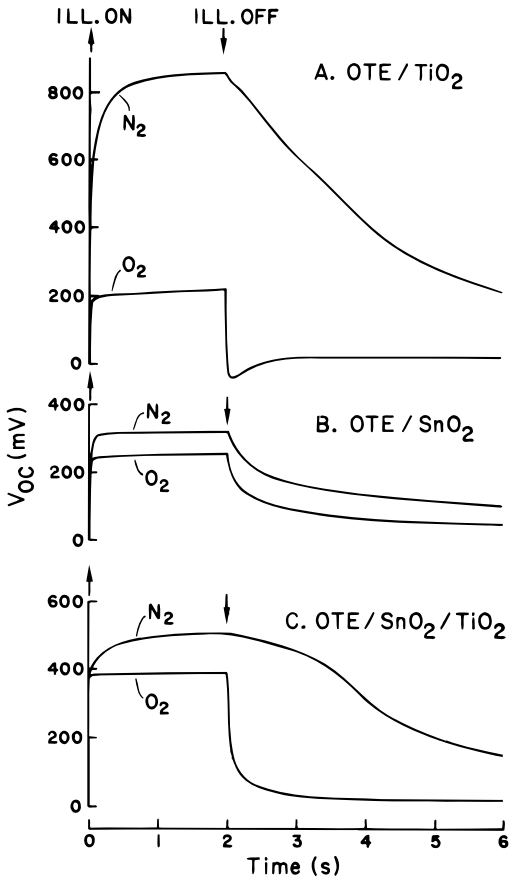

Figure 3. Open-circuit photovoltage response of (A) OTE/TiO_2, (B) OTE/SnO_2, and (C) OTE/SnO_2/TiO_2 (RE: SCE) to UV illumination. The electrolyte (0.02 M NaOH was saturated with (a) N_2 and (b) O_2. (The composition of composite semiconductor film was 0.18 mg/cm^2 of SnO_2 and 0.18 mg/cm^2 of TiO_2.)

lower in energy, cannot efficiently participate in the reduction of O_2 ($E_{CB} = -0.3$ V vs NHE).

Scavenging of electrons by O_2 plays an important role in promoting the photocatalytic oxidation in slurry systems as it suppresses electron accumulation within the particle and thus decreases the probability of electron−hole recombination. More detailed discussion of this topic can be found elsewhere.[26,29,30,32] It is noteworthy that even the presence of a small amount of SnO_2 makes the photovoltage of the SnO_2/TiO_2 composite films less sensitive to oxygen.

***i*−*V* Characteristics.** The *i*−*V* characteristics of OTE/TiO_2 electrode is compared with that of OTE/SnO_2/TiO_2 in Figure 4. Under negative bias, electron accumulation occurs in these particles. The optical effects arising as a result of such accumulation in TiO_2, SnO_2, and WO_3 particulate films have been studied earlier.[71,74−77] Under illumination with monochromatic light (320 nm), the OTE/TiO_2 electrode exhibits anodic photocurrent. The photocurrent increases with increasing anodic bias which is expected from the behavior of an n-type semiconductor.

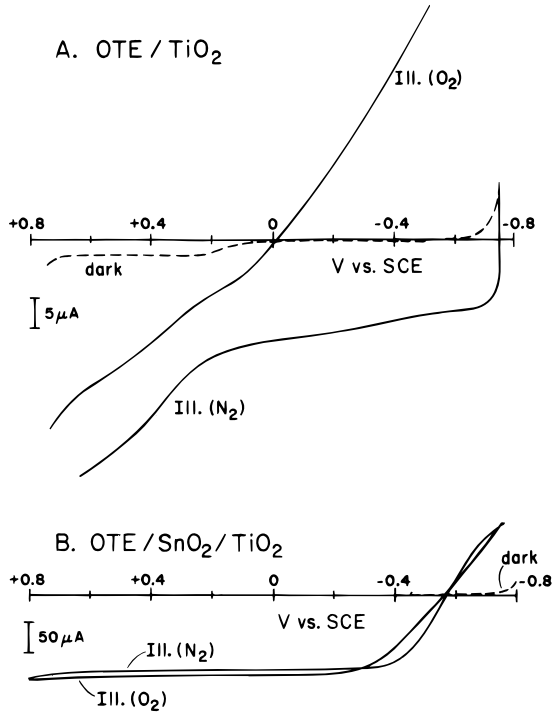

Figure 4. *i*−*V* characteristics of (A) OTE/TiO_2 (from ref 30) and (B) OTE/SnO_2/TiO_2 (RE: SCE, scan rate 5 mV/s) in (a) N_2- and (b) O_2-saturated aqueous solutions of 0.05 M NaOH. (The composition of composite semiconductor film was 0.30 mg/cm^2 of SnO_2 and 0.06 mg/cm^2 of TiO_2.) The traces were recorded in dark and under illumination with UV light.

Although, the generation of a space charge layer is not feasible in a 30 nm size particle, it is evident from the *i*−*V* characteristics that at positive bias the electrons are quite efficiently transported toward OTE surface while holes migrate to the electrode/electrolyte interface. As indicated earlier, the n-type semiconducting behavior is based on preferential hole injection into the electrolyte.[30,60,70−73] The application of an anodic bias to an OTE/TiO_2 electrode provides the necessary energy gradient to drive away the photogenerated holes and electrons in different directions and thus minimizes charge recombination. Application of this simple logic of achieving better charge separation in particles can be important in improving the efficiency of photocatalytic degradation of organic contaminants.

Another interesting behavior of the *i*−*V* characteristics is the observation of a zero-current at a potential in the range −0.2 to −0.4 V. This potential, which is close to the flat-band potential of the metal oxide semiconductor, indicates that all the photogenerated charge carriers are lost in the recombination process at this potential. Under illumination, this zero-current potential for OTE/TiO_2 shifts to positive potential (by ∼0.7 V) when the solution is saturated with O_2. This is attributed to the reduced O_2, which is formed during electron-scavenging reaction at the TiO_2 surface. The lack of an ideal space charge layer in these films makes the electrons recombine or react with adsorbed oxygen species during their transport to the collecting surface of OTE.[26,29,30,60,72,78,79]

Surprisingly no significant shift in the flat-band potential is observed for the OTE/SnO_2 or the composite film electrode, OTE/SnO_2/TiO_2. The presence of SnO_2

(74) O'Regan, B.; Grätzel, M.; Fitzmaurice, D. *Chem. Phys. Lett.* **1991**, *183*, 89.
(75) Hagfeldt, A.; Vlachopoulos, N.; Grätzel, M. *J. Electrochem. Soc.* **1994**, *141*, L82.
(76) Hotchandani, S.; Bedja, I.; Fessenden, R. W.; Kamat, P. V. *Langmuir* **1994**, *10*, 17.
(77) Bedja, I.; Hotchandani, S.; Carpentier, R.; Vinodgopal, K.; Kamat, P. V. *Thin Solid Films* **1994**, *247*, 195.
(78) Vinodgopal, K.; Kamat, P. V. *Sol. Energy Mater. Sol. Cells* **1995**, *38*, 401.
(79) Hagfeldt, A.; Bjorksten, U.; Lindquist, S. E. *Sol. Energy Mater. Sol. Cells* **1992**, *27*, 293.

Table 1. Photoelectrochemical Properties (Short-Circuit Photocurrent, i_{sc}, and Open-Circuit Photovoltage, V_{oc}) of Composite Semiconductor Films at Different Relative Compositions[a]

mass fraction of SnO_2 in mixture	mass fraction of TiO_2 in mixture	O_2 satd solution		N_2 satd solution		
		i_{sc} (μA)	V_{OC} (mV)	i_{sc} (μA)	V_{OC} (mV)	$(V_{OC}(O_2)-V_{OC}(N_2))$
1.0	0	9	250	4	320	−70
0.83	0.17	90	600	20	500	100[b]
0.67	0.33	100	475	23	550	−75
0.5	0.5	100	400	25	500	−100
0.17	0.83	22.5	630	20	800	−270
0	1.0	2	200	8.5	850	−650

[a]The total weight of semiconductor was kept constant at 0.36 mg/cm^2. The electrolyte was 0.02 M NaOH. Steady-state irradiation with $\lambda > 300$ nm. [b] The higher photovoltage observed in O_2-saturated solution is attributed to the effect of adsorbed oxygen on the photoelectrochemical properties which is more significant at this composition.

in the composite semiconductor film makes its photoelectrochemical response less sensitive to oxygen as photogenerated electrons are quickly accumulated in the SnO_2 nanocrystallites.

Effect of O_2 on the Photoelectrochemical Performance of Composite Systems. To further assess the effect of composition of two semiconductor colloids in the composite film, we monitored the short-circuit photocurrents and open-circuit photovoltages at different ratios of SnO_2 to TiO_2, while keeping the total mass of the catalyst constant. The results are summarized in Table 1. The effects of O_2 on the short-circuit photocurrent and open-circuit photovoltage becomes less pronounced as we increase the concentration of SnO_2 in the composite film. As described in earlier sections, this is due to the fact that electrons from TiO_2 are quickly transferred to SnO_2 crystallites before they can react with surface adsorbed oxygen.

We have recently shown that improved charge separation in a TiO_2-capped SnO_2 colloidal system results in increased hole trapping at the TiO_2 layer.[53] It has been shown earlier that the charge separation between two coupled semiconductor colloids could occur in few picoseconds.[44,46,55] If the charge separation was not instantaneous, electrons accumulated on TiO_2 particles would be scavenged by O_2. Varying degree of electron accumulation (n_c) alters the pseudo-Fermi level (E'_F) of the SnO_2−TiO_2 composite system. For an intrinsic type semiconductor we can express E'_F by the expression[80]

$$E'_F = E_{CB} + kT \ln(n_c/N_c) \qquad (2)$$

where N_c is the carrier density. V_{OC} in N_2 gives an estimate of maximum accumulation of electrons, while in O_2 it gives an estimate of electrons that are not scavengable by O_2. Therefore the difference between the two photovoltages $(V_{OC}(O_2)-V_{OC}(N_2))$ should give an estimate of the fraction of electrons that cannot be scavenged by O_2 in a semiconductor system. For TiO_2 alone, this difference is significant since most of the accumulated electrons are scavenged by O_2. On the other hand SnO_2 shows little difference in V_{OC} between O_2 and N_2 atmospheres. Since the charge separation in a composite system would result in accumulation of electrons on the SnO_2 particles, one would expect the effect of O_2 to be less on V_{OC} in the SnO_2/TiO_2 film.

To further assess the photocatalytic activity of nanostructured semiconductor films and to investigate whether this enhanced charge separation as evidenced

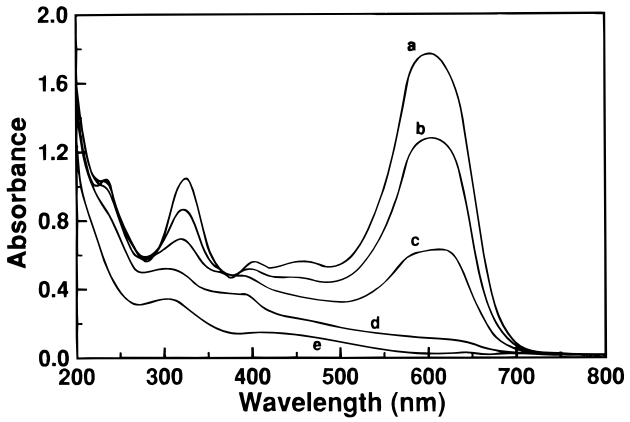

Figure 5. Absorption spectrum of a 37 ppm. (0.2 mM) naphthol blue black azo dye solution recorded at different time intervals following electrochemically assisted photocatalysis at an OTE/(SnO_2/TiO_2) electrode (0.30 mg/cm^2 of SnO_2 and 0.06 mg/cm^2 of TiO_2). The OTE/(SnO_2/TiO_2) electrode was maintained at an anodic bias of 0.8 V vs SCE and the solution was continuously bubbled with a slow stream of nitrogen. The absorption spectra were recorded at time intervals of (a) 0, (b) 10, (c) 30, (d) 60, and (e) 90 min.

from the photoelectrochemical measurements is reflected in more efficient degradation rates, we measured photocatalytic degradation rates of the blue azo dye NBB using the composite metal oxide film coated electrodes at various compositions of the two semiconductors.

Photocatalytic Degradation of NBB at OTE/SnO_2/TiO_2 Electrode. As shown in our preliminary study, the immobilized TiO_2 and SnO_2 particles are very effective in the degradation of azo dyes when used as a photoanode in a photoelectrolysis cell.[64] The advantages of these semiconductor particulate films are that (a) oxygen is not essential to scavenge the photogenerated electrons since efficient charge separation of the photogenerated electrons and holes can be achieved by applying an anodic bias potential to the immobilized semiconductor particulate film and (b) the rate of degradation is enhanced as the applied anodic potential is increased from 0 to +0.8 V. The major photoelectrochemical reactions that initiate redox processes in the electrode compartments can be summarized as follows:

$$\text{At photoanode:} \quad SnO_2/TiO_2 + h\nu \longrightarrow \underbrace{\{SnO_2(\mathbf{e}...\mathbf{h})\}\{TiO_2(\mathbf{e}...\mathbf{h})\}}$$

$$\downarrow$$

$$SnO_2(\mathbf{e}) + TiO_2(\mathbf{h}) \qquad (3)$$

$$TiO_2(\mathbf{h}) + OH^- \rightarrow TiO_2 + OH^\bullet \qquad (4)$$

$$TiO_2(\mathbf{h}) \text{ or } OH^\bullet + NBB \rightarrow \text{products} \qquad (5)$$

$$\text{At dark cathode:} \quad Pt(2\mathbf{e}) + O_2 + 2H^+ \rightarrow H_2O_2 \qquad (6)$$

The absorption spectra of an aqueous solution of NBB recorded following the excitation of an OTE/SnO_2/TiO_2 are shown in Figure 5. The OTE/SnO_2/TiO_2 is maintained at a positive bias of 0.8 V vs SCE to facilitate efficient charge separation in the semiconductor film. The oxidation potential of NBB is determined to be 1.0 (±0.05) V at a glassy carbon electrode vs SCE. Therefore the choice of 0.8 V as an applied bias potential in these electrochemically assisted photocatalytic experiments ensured that no direct oxidation of NBB occurred

during these experiments. The solution was continuously bubbled with a stream of nitrogen so that electrochemically assisted photocatalysis could be carried out under anaerobic conditions. It should be noted that NBB is a photostable dye which undergoes negligible photodegradation when exposed to light ($\lambda > 300$ nm) in the absence of a semiconductor particulate film.

As can be seen from Figure 5, the absorption peaks corresponding to the blue dye disappear completely following photolysis of the semiconductor film. Even more surprising is the relative speed with which the dye degradation can be achieved. An aqueous solution of 37 ppm dye is 67% degraded following 30 min of irradiation of the semiconductor electrode indicating a pseudo-first-order rate constant, k, of 3.6×10^{-2} min^{-1}. For comparison, an electrochemically assisted photocatalysis experiment was also carried out with NBB dye solution using OTE, OTE/SnO_2, and OTE/TiO_2 separately under identical conditions (i.e., at an anodic bias of +0.8 V vs SCE and with nitrogen gas bubbling). Negligible degradation of the dye occurred with the blank OTE electrode. However the observed pseudo-first-order degradation rate constants of the OTE/SnO_2 and OTE/TiO_2 electrode were similar ($k = 1.1 \times 10^{-2}$ min^{-1}) but about 3 times slower than the OTE/SnO_2/TiO_2 system. (The total mass of the semiconductor on the electrode was the same in all three cases (0.36 mg/cm^2).) Similar enhancement (10 times) in the degradation rate was also observed for the degradation of another textile dye, acid orange 7 at an SnO_2/TiO_2 composite film electrode.[64] These results highlight the role of composite semiconductor films in enhancing the photocatalytic degradation rates of azo dyes.

The rapid disappearance of the 615 nm absorption band in Figure 5 suggests that the chromophore responsible for the characteristic color of the azo dye is breaking down. Earlier studies on similar dyes by our group and others have shown that the dye is cleaved at the azo bond.[64,81,82] It is expected that the intermediates generated during such a process can also undergo hydroxyl radical induced oxidative degradation. Evidence suggesting that such a degradation is occurring in our electrochemically assisted photocatalytic experiments is seen in the absorption spectra (Figure 5) where all the absorption bands of the blue dye including those between 200 and 300 nm are significantly affected and reduced. The speed with which decolorization is achieved compares very favorably with other reported results of hydroxyl radical mediated degradation of azo dyes.[82]

Effect of Externally Applied Bias on the Rate Constant of Photocatalytic Degradation. As an illustration of the effectiveness of electrochemically assisted photocatalysis in general, we measured the degradation rates of NBB using the composite semiconductor film electrodes in nitrogen-saturated solutions as a function of the applied anodic bias voltage (Figure 6). When no external potential is applied, very little degradation is observed. At an anodic bias of +0.4 V the dye decays with a pseudo-first-order rate constant of 1.6×10^{-2} min^{-1}. When the potential is increased to +0.8 V, the rate constant of NBB degradation increases ($k = 3.6 \times 10^{-2}$ min^{-1}).

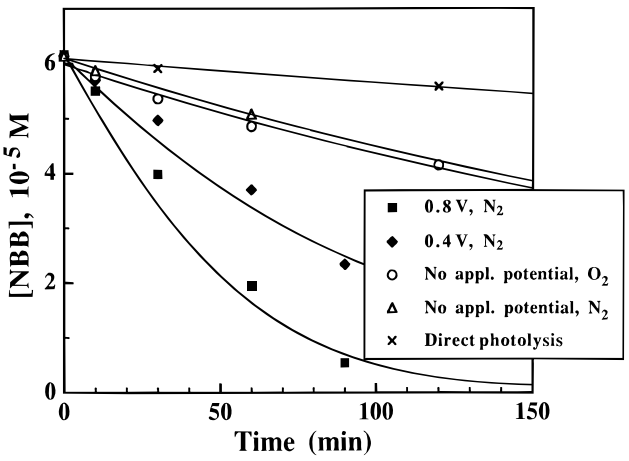

Figure 6. Dependence of NBB degradation on the externally applied anodic bias. The OTE/(SnO_2/TiO_2) composition is the same as in Figure 5 and was maintained at (a) no applied potential in N_2 (△) and (b) no applied potential in O_2 (○), (c) 0.4 V, (♦), and (d) 0.8 V (■) vs SCE, during the photolysis. As in (a), for (c) and (d) the solution in the working electrode compartment was continuously bubbled with a slow stream of nitrogen. The results of the blank experiments (×) carried out with direct photolysis using OTE electrode (without the catalyst film) is also shown.

We also studied the degradation of NBB using a SnO_2/TiO_2 composite film coated on the OTE but with no applied potential and oxygen gas bubbling through the solution. Such a setup is similar to the conditions employed in a typical photocatalysis experiment in which a photocatalyst is immobilized on a glass or fiber surface. The degradation rate of NBB was quite slow with a pseudo-first-order rate constant of 0.23×10^{-2} min^{-1} (Figure 6). We also carried out appropriate control experiments to confirm the observation that the enhancement in the degradation rate is truly a photocatalytic effect arising from the composite semiconductor electrode. At a bias potential of +0.8 V, with no illumination, no degradation was observed in either nitrogen or oxygen saturated solutions. This further affirms that at a bias potential of +0.8 V, direct oxidation of the dye does not occur at the semiconductor electrode.

Optimization of SnO_2 and TiO_2 Composition. Efforts were made to optimize the ratio of the two semiconductors that is necessary to obtain the maximum rate of NBB degradation. The specific aim is to investigate whether the enhancement of charge separation resulting from the coupling of the two systems TiO_2 and SnO_2 is reflected in more efficient degradation of NBB. Figure 7 is a bar diagram which shows the degradation rates obtained for NBB using the composite semiconductor system in which the mass of SnO_2 is kept constant at 0.36 mg/cm^2, but the amount of TiO_2 is increased progressively from 0 to 0.4 mg/cm^2. Higher loadings of TiO_2 do seem to slow the degradation process primarily due to the increased opacity of the resulting films. The best enhancement in photocatalytic activity is generally seen when the amount of SnO_2 is higher than TiO_2 in the composite.

As in the photoelectrochemical experiments, we also measured decay rates of NBB at different ratios of SnO_2 to TiO_2 keeping the total mass of the catalyst constant. A comparison of the relative degradation rates under these conditions but with four different compositions of SnO_2 and TiO_2 is shown in Figure 8. All the degrada-

(80) Myamlin, V. A.; Pleskov, Y. V. *Electrochemistry of semiconductors*; Plenum Press: New York, 1967.
(81) Matsui, K.; Shikata, K.; Takase, Y. *Dyes Pigments* **1984**, *5*, 325.
(82) Spadaro, J. T.; Isabelle, L.; Ranganathan, V. *Environ. Sci. Technol.* **1994**, *28*, 1389.

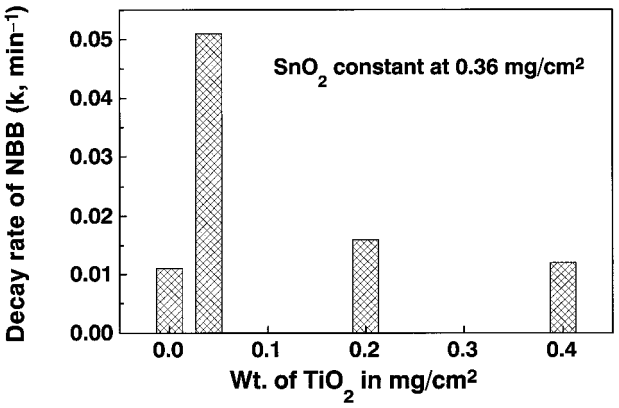

Figure 7. Dependence of the photocatalytic degradation rate of NBB on the TiO_2 concentration in the composite system. The weight of SnO_2 in the composite system was kept constant at 0.36 mg/cm^2. The bias potential was 0.8 V vs SCE and the electrolyte was 37 ppm NBB in water at unbuffered pH 5.

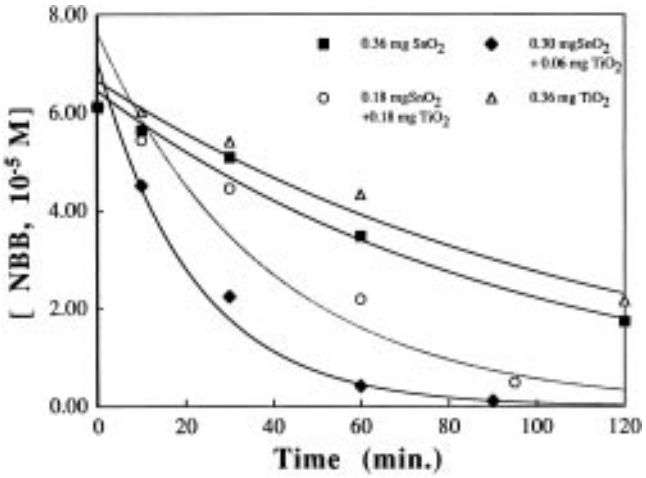

Figure 8. Dependence of NBB degradation rate on the nature of semiconductor film; (a) OTE/SnO_2 (0.36 mg/cm^2 (■), (b) OTE/(0.30 mg of SnO_2/0.06 mg of TiO_2/cm^2) (♦), (c) OTE/(0.18 mg SnO_2/0.18 mg TiO_2/cm^2) (○), and (d) OTE/TiO_2 (0.36 mg/cm^2) (△). The electrodes were maintained at a bias potential of 0.8 V vs SCE. In all of these experiments nitrogen was bubbled through the dye solution (pH 5, unbuffered).

tion rates were measured under identical conditions, i.e., applied potential of 0.8 V, N_2-saturated solutions and the same excitation intensity. It is clear from Figure 8, that degradation is rapid with the composite systems, but the fastest rates are obtained when the mass ratio of SnO_2 to TiO_2 is at least 2:1 or higher. The more significant observation from these kinetic plots is that these decay rates show a very strong correlation with difference in photovoltage ($V_{OC}(O_2)-V_{OC}(N_2)$). In Figure 9 we have plotted the difference in photovoltage and the degradation rates of NBB against the mass fraction of SnO_2 in the composite mixture. (Note that the total weight of the semiconductor mixture was maintained constant.) The decay rate of NBB shows a maximum at a composition of 83% SnO_2 in the mixture. At this composition the oxygen has a minimum effect on the photovoltage. In fact the photovoltage observed at this composition is slightly higher than in N_2 atmosphere. This is attributed to the effect of adsorbed oxygen on the photoelectrochemical properties of the semiconductor film.[30,83]

(83) Hagfeldt, A.; Lindstrom, H.; Sodergren, S.; Lindquist, S. E. *J. Electroanal. Chem.* **1995**, *381*, 39.

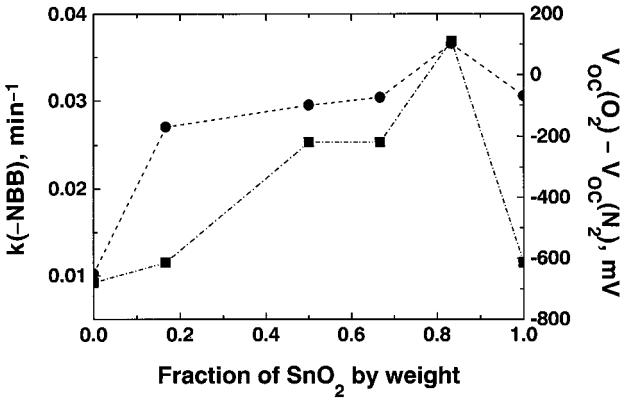

Figure 9. Dependence of the photocatalytic degradation rate of NBB on the fraction of SnO_2 (by weight) in the OTE/SnO_2/TiO_2 system. The total weight of semiconductor was kept constant at 0.36 mg/cm^2. Also plotted on the right *Y* axis is the difference in photovoltage between O_2- and N_2-saturated solutions.

Under UV excitation, charge separation occurs in closely contacted pairs of SnO_2 and TiO_2 particles. Since the electrons and holes quickly move in opposite directions to accumulate on SnO_2 and TiO_2 particles respectively, their recombination is greatly suppressed. This is reflected in the higher photon-to-photocurrent conversion efficiencies for SnO_2/TiO_2 composite films and also manifested in the enhancement of photocatalytic degradation abilities. It should be noted that SnO_2 particles are smaller (particle diameter 3−5 nm) than TiO_2 (particle diameter 30 nm). Thus, even at 1:1 composition (by weight) of the two semiconductor particles we would expect each TiO_2 particle to be surrounded by hundreds of SnO_2 particles. This was also confirmed from the SEM picture in Figure 1c. Such a configuration is likely to favor quick electron transfer from excited TiO_2 into SnO_2 particles and their transport toward the collecting surface of OTE. The holes that remain on the TiO_2 particles are efficiently utilized in the oxidation of the dye molecules.

To make the composite SnO_2/TiO_2 system useful for photocatalysis, it is essential to carry out these experiments with an externally applied electrochemical bias. It provides necessary potential gradient within the nanostructured semiconductor film to drive away the accumulated electrons via the external circuit and thus promote oxidation at the semiconductor/electrolyte interface. The results presented here highlight the usefulness of a SnO_2/TiO_2 composite semiconductor thin films for enhancing the rate of photocatalytic degradation process. We are currently carrying out HPLC analyses to determine the nature of the intermediates and the mechanism with which these intermediates influence overall mineralization process.

Acknowledgment. We would like to thank Richard Frankovic, Department of Electrical Engineering, for his assistance in recording SEM pictures. K.V. acknowledges the support of Indiana University Northwest through a Grant-in-Aid. P.V.K. acknowledges the support of the Office of Basic Energy Sciences of the Department of Energy. This is Contribution No. NDRL-3837 from the Notre Dame Radiation Laboratory.

CM950425Y